Spatial correlation between brain aerobic glycolysis and amyloid-β (Aβ) deposition

Andrei G. Vlassenko[a], S. Neil Vaishnavi[a], Lars Couture[a], Dana Sacco[a], Benjamin J. Shannon[a], Robert H. Mach[a], John C. Morris[b], Marcus E. Raichle[a,b,c,d,1], and Mark A. Mintun[a,1]

Departments of [a]Radiology, [b]Neurology, [c]Neurobiology, and [d]Biomedical Engineering, Washington University School of Medicine, St. Louis, MO 63110

Contributed by Marcus E. Raichle, August 9, 2010 (sent for review July 28, 2009)

Amyloid-β (Aβ) plaque deposition can precede the clinical manifestations of dementia of the Alzheimer type (DAT) by many years and can be associated with changes in brain metabolism. Both the Aβ plaque deposition and the changes in metabolism appear to be concentrated in the brain's default-mode network. In contrast to prior studies of brain metabolism which viewed brain metabolism from a unitary perspective that equated glucose utilization with oxygen consumption, we here report on regional glucose use apart from that entering oxidative phosphorylation (so-called "aerobic glycolysis"). Using PET, we found that the spatial distribution of aerobic glycolysis in normal young adults correlates spatially with Aβ deposition in individuals with DAT and cognitively normal participants with elevated Aβ, suggesting a possible link between regional aerobic glycolysis in young adulthood and later development of Alzheimer pathology.

Alzheimer's disease | default mode network | positron emission tomography

Cerebral amyloid-β (Aβ) plaque deposition is a hallmark of Alzheimer's disease (AD) (1, 2), and there is clinical pathological evidence that Aβ deposition may precede clinical manifestation of cognitive deficits and dementia of the Alzheimer type (DAT) (3, 4). However, it is unclear whether the site and extent of Aβ deposition is related to any preceding pattern of brain activity or metabolism.

A radiotracer with high affinity to Aβ plaques, N-methyl-[^{11}C] 2-(4′-methylaminophenyl)-6-hydroxybenzothiazole (or ^{11}C-PIB, for "Pittsburgh Compound-B"), has been developed for PET study and has demonstrated substantially increased regional uptake in individuals with DAT and also in some cognitively normal older persons (5–7). The spatial distribution of Aβ plaques by PET imaging in individuals with DAT appears strikingly similar to the default mode network (DMN), a group of brain regions that are more active when normal individuals are not engaged in attention-demanding, goal-directed task performance (8–10).

The unique distribution of Aβ in DAT suggests that something unique to these brain areas predisposes them to the pathophysiology of AD (9, 11). One of the many features of these areas is their reliance on glucose outside its usual role as substrate for oxidative phosphorylation (12). In adequately oxygenated tissue, this use of glucose usually is referred to as "aerobic glycolysis" and accounts for 10–15% of the glucose metabolized by the brain (13–15). It should be noted that the term "aerobic glycolysis" includes glycolysis itself (metabolism of glucose-6-phosphate to pyruvate) as well as glucose entering the pentose phosphate shunt and glycogen synthesis.

Because many critical functions are associated with glucose outside its traditional role in supplying energy through oxidative phosphorylation (16–19), this relationship might signal a causal element in the chain of events leading to DAT. As a first step in exploring this possibility, we wanted to confirm the apparent spatial relationship between DAT and those brain systems uniquely reliant on aerobic glycolysis. We did so by comparing the distribution of aerobic glycolysis in normal young adults with the distribution of Aβ plaques in individuals with DAT and in cognitively normal participants with a high level of Aβ deposition. Our results confirm a striking spatial correspondence.

Results

Aerobic glycolysis traditionally is assessed in terms of the molar ratio of oxygen consumption to glucose utilization, the oxygen–glucose index (OGI). When all the glucose metabolized is converted to carbon dioxide and water, the OGI is 6. A number less than 6 indicates that aerobic glycolysis is present. In our companion study (12) we estimated aerobic glycolysis in this traditional manner by the voxelwise division of relative cerebral metabolic rate for oxygen ($CMRO_2$) by the relative cerebral metabolic rate for glucose (CMRGlu) and scaling the resulting quotient imaging to obtain a whole-brain molar ratio of 5.3, based on earlier published work (13–15).

Although the OGI is a straightforward measure based on well-established metabolic principles, OGI images may be noisy in areas of low metabolism because they involve voxelwise division. Also, the value of the OGI is inversely related to the degree of aerobic glycolysis, a relationship sometimes confusing to readers. To overcome these limitations, we defined here and in our companion paper (12) a different measure of aerobic glycolysis in the brain: the glycolytic index (GI). The GI is obtained by linear regression of CMRGlu on $CMRO_2$ (12) and exhibiting the residuals scaled by 1,000. Positive GI values represent more aerobic glycolysis, and negative GI values represent less glycolysis than predicted by the line of regression. The two measures of aerobic glycolysis, OGI and GI, are highly correlated in our data ($r = -0.913$, $P < 0.001$) (12). For descriptive purposes in this paper we use the GI.

Two different strategies were used in parsing the brain for the analysis of correlation between PET measures of energy metabolism and Aβ deposition. One approach was to cover the whole-brain image with 167 nonoverlapping 14-mm isotropic cubes. The second approach used 60 spheres, 6 mm in diameter, placed in different brain regions including frontal, temporal, parietal, and occipital cortex as well as in the cerebellum, subcortical structures, and white matter (Tables S1–S3). All volumes of interest were applied to average ^{11}C-PIB binding potential (BP) (details are given in *Methods*), GI, CMRGlu, $CMRO_2$, and cerebral blood flow (CBF) image and values were used for the analysis of Pearson correlation.

Using nonoverlapping cubes, we found strong correlations between ^{11}C-PIB binding and aerobic glycolysis both for individuals with DAT ($r = 0.70$, $P < 0.0001$, Pearson correlation) (Fig. 1*A*) and for cognitively normal ^{11}C-PIB–positive participants ($r = 0.43$, $P < 0.0001$, Pearson correlation) (Fig. 1*B*). For each cube, we sub-

Author contributions: M.E.R. and M.A.M. designed research; A.G.V. and S.N.V. performed research; R.H.M. contributed new reagents/analytic tools; A.G.V., S.N.V., L.C., D.S., B.J.S., J.C.M., and M.E.R. analyzed data; M.E.R. wrote the paper; and J.C.M. was responsible for patient selection.

The authors declare no conflict of interest.

Data deposition: NP721 data available on request (https://cnda.wustl.edu/).

Freely available online through the PNAS open access option.

See Commentary on page 17459.

[1]To whom correspondence may be addressed. E-mail: marc@npg.wustl.edu or minturnm@mir.wustl.edu.

This article contains supporting information online at www.pnas.org/lookup/suppl/doi:10.1073/pnas.1010461107/-/DCSupplemental.

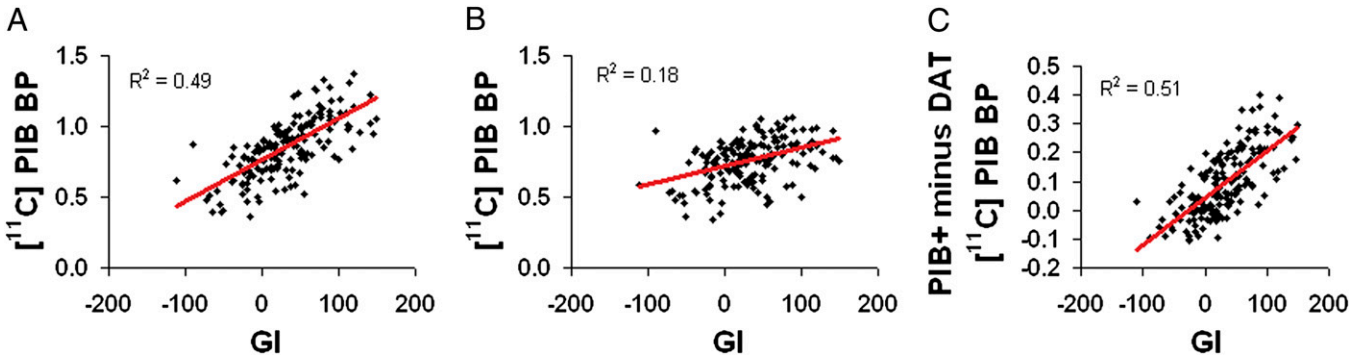

Fig. 1. Measurements of ^{11}C-PIB BP (displayed on the *y* axis) were performed in 11 individuals with DAT (*A*) and in 14 cognitively normal community-dwelling individuals (*B*) and, in both cases, were compared with the level of aerobic glycolysis measured in 33 neurological control individuals (*x* axis). The level of aerobic glycolysis (GI) represents the amount of glucose consumption above or below that predicted by the amount of oxygen. (Further details are given in the text and in ref. 12.) These data were obtained from 167 nonoverlapping isotropic cubes covering the whole brain that were normalized to the ^{11}C-PIB binding potential cerebellum. (*C*) The difference between ^{11}C-PIB values in DAT and cognitively normal groups was calculated and plotted against the GI. The strong positive correlation indicates that, although the regional pattern of Aβ distribution remains similar, the slopes of the relationships depicted in *A* and *B* differ significantly ($P < 10^{-4}$).

tracted the ^{11}C-PIB values of the DAT group from those of the cognitively normal group. The difference between groups increases with increasing GI, indicating that the ^{11}C-PIB/GI relationship is stronger, and the slope is steeper, for the DAT group ($P < 0.0001$) (Fig. 1*C*). The spatial relationships implied by these correlations are visually dramatic (Fig. 2). Correlations were comparatively lower between ^{11}C-PIB BP and the CMRGlu ($r = 0.20$, $P < 0.001$ and $r = 0.18$, $P < 0.05$, respectively, for DAT and cognitively normal participants).

Using the regionally placed spheres (Tables S1–S3) we also found the strongest correlations between ^{11}C-PIB BP and GI for DAT ($r = 0.74$, $P < 0.0001$; Pearson correlation) and cognitively normal ^{11}C-PIB–positive participants ($r = 0.55$, $P < 0.0001$; Pearson correlation), whereas the correlation between ^{11}C-PIB BP and CMRGlu was substantially lower for individuals with DAT ($r = 0.44$, $P < 0.001$ for CMRGlu; $r = 0.16$, Pearson correlation) and was not significant for cognitively normal ^{11}C-PIB–positive participants ($r = 0.16$, Pearson correlation).

The correlations between ^{11}C-PIB and $CMRO_2$, oxygen extraction fraction, and CBF were not significant in either group.

Discussion

Changes in brain metabolism in the distribution of the DMN in DAT have been noted for some time (for the earliest observation, see refs. 20 and 21). More recently (22, 23) changes in metabolism have been examined in relation to amyloid burden in individuals with DAT as measured with ^{11}C-PIB. Two aspects of these observations should be noted. First, in all these reports the clinical diagnosis of DAT was already established, making the role of metabolic changes ambiguous (i.e., the metabolic changes are as likely to be a consequence of the disease as a causal factor). Second, in all these reports metabolism has been measured with PET using ^{18}F-fluorodeoxyglucose (FDG) uptake and retention. It is important to understand why exclusive reliance on this tracer limits the information available with regard to the role of glucose in AD.

FDG-PET is a well-established technique for the quantitative measurement of regional brain glucose metabolism in humans (24, 25). The FDG technique is used almost universally in brain research with the tacit assumption that the glucose utilization measures energy metabolism via oxidative phosphorylation. However, the FDG technique measures only the first step in glucose metabolism, the phosphorylation to glucose-6-phosphate by hexokinase. Because the majority of glucose entering the adult human brain is metabolized ultimately to water and carbon dioxide via oxidative phosphorylation, ignoring the other potential fates of glucose has been accepted as an operational convenience, with few interpretive consequences, when using FDG-PET. However, as demonstrated first in Huntington's disease (15) and now in our

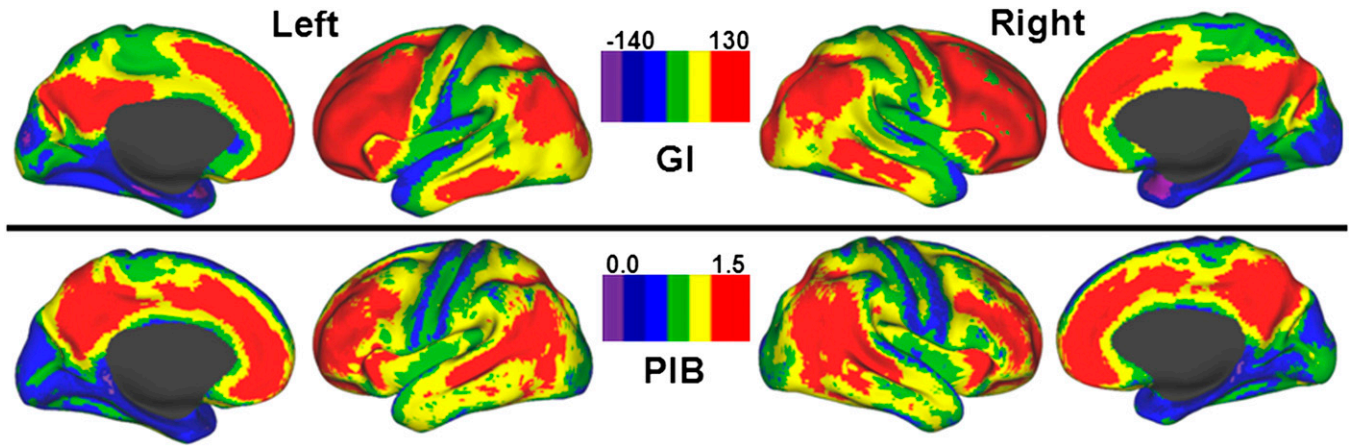

Fig. 2. Maps showing lateral and medial cortical surfaces of the human brain on which are depicted the mean distribution of aerobic glycolysis in units of the GI in 33 neurologically normal young adults and ^{11}C-PIB BP in 11 individuals with DAT. The GI corresponds to the amount of glucose consumption above or below that predicted by the amount of oxygen consumed. (Further details are given in the text and in Fig. 1.)

data, probing the metabolic fate of glucose in more detail may be important in understanding the pathophysiology of Huntington's disease, AD, and other diseases as well.

Our data indicate that when Aβ accumulates in the human brain in AD, it does so in a distribution that closely mirrors that of elevated aerobic glycolysis in the resting state of healthy young adults. These elevated levels of aerobic glycolysis, defined in this study as levels of aerobic glycolysis significantly above the brain mean, are not just the consequence of elevated levels of overall energy metabolism (9). For example, primary visual cortex shows a very high level of glucose utilization and the highest levels of oxygen utilization (the primary measure of energy consumption), which in the primary visual cortex of the normal adult human is 35% above the brain mean (12). However, primary visual cortex accumulates low levels of Aβ and exhibits a minimal decline in glucose utilization in DAT (12, 26, 27). The level of aerobic glycolysis in primary visual cortex is at the brain mean (tables 1 and 2 in ref. 8 and our companion paper, ref. 12.) Thus, the DMN is distinguished primarily by its reliance on aerobic glycolysis and not by overall energy consumption. A significantly elevated overall level of energy consumption is seen principally in the posterior cingulate cortex and adjacent medial precuneus (tables 1 and 2 in ref. 8 and our companion paper, ref. 12).

An initial motivating factor in our studies of aerobic glycolysis was that it increased in brain areas exhibiting task-induced activity (28). It was shown later by others that this task-induced activity could persist following the completion of task performance (29). Reinforcing our interest in aerobic glycolysis was work, largely conducted in oncology, showing the importance of aerobic glycolysis in proliferating cells (the "Warburg effect" named after its discoverer, ref. 30); ref. 16 gives a current perspective.) Because even normal cells, when proliferating, resort to aerobic glycolysis (31), we wondered whether in the normal brain aerobic glycolysis, which nominally represents 10–15% of the glucose use in the adult human (13–15), might represent a unique biomarker of cellular events associated with brain development in fetuses and newborns (32) and daily, activity-dependent synaptic changes (i.e., redevelopment) in adults (33). (For a cell biology perspective, see ref. 34.) Support for this hypothesis comes from available human data.

In preterm infants more than 90% of the glucose used is consumed outside oxidative phosphorylation (35, 36). By term, this fraction accounts for 35% of the glucose used by the brain (37), compared with 10–12% in adults (13–15). During the first decade of life overall glucose metabolism reaches levels twice that of adults before returning gradually to adult levels over the second decade (38). Unfortunately, these latter data provide no information on aerobic glycolysis, because only glucose metabolism was measured, but it seems reasonable to assume that this doubling of brain glucose consumption in the first decade of life does not represent a doubling of the energy consumption of an already very expensive organ (12, 39). In adults, whole-brain aerobic glycolysis almost doubles to 19% from 11% as the result of a day's waking (14). This increase is reset after a night's sleep (14).

Taken together these observations in children and adults suggest that glucose, apart from its use as substrate for oxidative phosphorylation, plays a role in the ongoing cellular dynamics of the brain. Brain areas such as the DMN indicate by their elevated levels of aerobic glycolysis a dependence that is related to their vulnerability to AD. Extant data suggest that a causal link between dependence on aerobic glycolysis and AD might emerge from a failure to sustain critical glucose-dependent synaptic functions as well as the glucose-dependent management of oxidative stress and biosynthesis of proteins, lipids, and nucleic acids. We review briefly the functions seemingly most relevant to AD.

Glucose is critical for the synapse in at least two ways. First, it is essential for the removal of glutamate into astrocytes from the synaptic cleft (40). Glutamate is cleared from the synapse by a sodium-coupled process. Sodium then must be removed from the astrocytes by Na/K-ATPase, a pump fueled by glycolysis in all cell systems in which it is found (41–45), probably because it delivers ATP at twice the rate of oxidative phosphorylation (46). Failure to remove glutamate efficiently from the synapse can be damaging because excessive glutamate acts as an excitatory neurotoxin (47, 48). It may be more than coincidental that earlier models of glutamate-induced excitotoxicity in rodents (49) exhibit lesion distributions strikingly similar to the distribution of Aβ in transgenic mouse models of AD (e.g., see ref. 50). Increased neuronal excitability and seizure activity in persons with DAT as well as in transgenic mouse models of AD (recently reviewed in ref. 51) might be the result of a failure to deal effectively with synaptic glutamate.

A second and related synaptic role for glucose takes place in the postsynaptic density (PSD) of dendritic spines, where the enzymatic machinery for glycolysis is located also (44). There glycolysis-fueled Na/K-ATPase regulates AMPA receptor turnover (52). Na/K-ATPase dysfunction leads to a loss of cell-surface expression of AMPA receptors and a depression in synaptic transmission (52). It has been posited that AMPA receptor removal underlies Aβ-induced synaptic depression and the loss of dendritic spines (53).

The phase of glycolysis delivering ATP to Na/K-ATPase in both astrocytes and the PSD is controlled by glyceraldehyde 3-phosphate dehydrogenase (G3PD). G3PD has been implicated genetically in the pathophysiology of late-onset AD (54–56) and, through disulfide bonding, can be inactivated by Aβ (56). Thus, a concentration-dependent, Aβ-induced interference with the delivery of ATP to Na/K-ATPase in astrocytes and the PSD could link elevated levels of Aβ to synaptic depression, the loss of dendritic spines, and glutamate-induced excitotoxicity. Because synaptic Aβ levels parallel those of glutamate (57–59) and exhibit an apparent concentration-dependent effect on synaptic physiology [i.e., facilitation at low concentrations (60, 61) and inhibition at high concentrations (53, 59, 62, 63)], abnormally elevated levels of both glutamate and Aβ might lead to a mutually reinforcing state of synaptic failure.

Apart from its role specifically in the synapses, glucose plays a critical role in protecting the brain against reactive oxygen species (ROS) and avoiding oxidative stress (31), putatively an important factor in the pathophysiology of AD (recently reviewed in ref. 64; also see ref. 65). Protection largely occurs when glucose-6-phosphate is diverted from glycolysis into the pentose phosphate pathway (PPP) by coordinated changes in the activities of phosphofructokinase-1 (PFK-1), the rate-limiting enzyme for glycolysis, and glucose-6-phosphate dehydrogenase (G6PDH), the rate-limiting enzyme for the PPP.

In the PPP reducing equivalents in the form of NADPH are provided to glutathione, the major nonenzymatic cellular antioxidant. Intracellular glutathione, with the help of nitric oxide (17), also maintains cytochrome *c* in a reduced and inactive state, thus inhibiting cytochrome *c*-induced apoptosis in neurons (18). The protective role of the brain PPP against ROS and apoptosis has been demonstrated in transgenic mice with increased expression of G6PDH when challenged with oxidative stress (66). Also, up-regulation of the PPP is a distinctive feature of surviving brain cells from individuals with DAT (67–69). It is noteworthy that G6PDH, the gatekeeper of the PPP, is the most common enzyme deficiency worldwide (70). Could G6PDH deficiency be a hidden risk factor for AD?

Diversion of glucose into the PPP involves a delicate cellular balancing act involving neurons and astrocytes (71) in which overall energy needs must be maintained properly through glycolysis (2 ATP for ion pumping and protein synthesis) and oxidative phosphorylation (30 ATP) while the cellular redox state is maintained by diverting glucose through the PPP. Recent research in cell biology suggests, surprisingly, that the PPP may be the preferred fate of glucose in neurons because of the low level of PFK-2, a key regulator of PFK-1 and hence glycolysis (72), and that altering this arrangement and increasing the flux through

glycolysis increases the susceptibility of neurons to oxidative stress. Management of these complex metabolic arrangements may depend heavily on astrocytes (71).

Astrocytes may provide neurons with lactate to supplement glycolysis in fueling oxidative phosphorylation (71, 72) and precursors of glutathione (73) that are released from the cell and made available to neurons for the management of ROS (71, 73, 74). When astrocytes take up Aβ, which in high concentrations aggregates within them, glycogen synthesis, oxidative phosphorylation, PPP activity, and the production of ROS all increase significantly (73). In the presence of astrocytes preexposed to Aβ, neuronal viability is significantly reduced.

Interestingly, the decrease in neuronal viability induced by exposing normal neurons to Aβ-treated astrocytes is abolished by inhibiting a key signaling cascade mediating the effect of insulin on glucose metabolism (73). Paradoxically, however, controlled hyperinsulinemia transiently improves memory performance in individuals with DAT (75). Such observations inject a note of caution about uncritically translating observations on cells harvested from immature animals to the in vivo situation in laboratory animals and humans. The reverse is true, also, as we argue in this paper. We must not uncritically interpret changes in brain glucose metabolism in AD, or the normal brain, as if they were a simple matter of overall energy metabolism and ignore the diverse role this remarkable molecule plays in the life of the brain. The complexities of transcending these levels of inquiry are challenging, but the rewards for doing so are likely to be great.

Finally, our data hint at ways in which AD might progress from subclinical disturbances in brain cell biology into the clinical phenotype. This suggestion emerges from a consideration of the difference in the relationship of ^{11}C-PIB BP and GI depicted in the correlations shown in Fig. 1. Both groups exhibit a strong relationship between GI and Aβ deposition. Strikingly, the regional patterns of Aβ deposition, and their relations to GI, are quite similar in the two groups. In fact, the groups differ primarily only in the total amount of Aβ deposition (Fig. 1*C*). This result suggests that the ^{11}C-PIB–positive, cognitively normal group is simply at an earlier stage of the pathological processes seen in the DAT group. It would be of interest to follow prospectively cognitively normal ^{11}C-PIB–positive individuals to determine whether the change in the slope of the relationship between ^{11}C-PIB BP and GI predicts which of these persons will develop the phenotype of DAT.

Methods

Participants. Thirty-three healthy, right-handed, neurologically normal participants (19 females and 14 males; mean age 25.4 ± 2.6 y) were recruited from the Washington University community and underwent blood flow and metabolic studies with PET. Individuals were excluded if they had contraindications to MRI, history of mental illness, possible pregnancy, or medication use that could interfere with brain function. Further details concerning these participants and their PET imaging studies are presented in our companion paper (12).

In addition 25 participants underwent ^{11}C-PIB studies with PET. Of these participants, 11 were individuals with DAT (7 females and 4 males; mean age 79.7 ± 5.0 y) selected for this study from participants enrolled in the Washington University Alzheimer's Disease Research Center (ADRC). In addition, 14 were cognitively normal community-dwelling individuals (9 females and 5 males; mean age 74.6 + 7.9 y), also enrolled in the ADRC who had high levels of ^{11}C-PIB deposition [i.e., a mean cerebral ^{11}C-PIB BP of 0.18 or greater (7)]. The clinical assessment protocol used in evaluating these subjects has been described previously (76).

All experiments were approved by the Human Research Protection Office and Radioactive Drug Research Committee at Washington University in St. Louis. Written informed consent was provided by all participants or their caregivers.

Structural MRI. MRI scans were obtained in all subjects to guide anatomical localization. High-resolution structural images were acquired using a 3D sagittal T1-weighted MPRAGE on a Siemens 3T Allegra (TE = 3.93 ms, TR = 1,900 ms, TI = 1,100 ms, flip angle = 20°, 256 × 256 acquisition matrix, 160 slices, 1 × 1 × 1 mm voxels) or 1.5T Sonata scanner (TE = 3.93 ms, TR = 1,900 ms, TI = 1,100 ms, flip angle =15 °, 224 × 256 acquisition matrix, 160 slices, 1 × 1 × 1 mm voxels).

PET Imaging. ^{11}C-PIB radiochemistry synthesis is described elsewhere (7).

^{11}C-PIB imaging. The ^{11}C-PIB imaging has been described in detail (7) and was conducted with a Siemens 961 HR+ ECAT PET scanner (Siemens/CTI). After positioning, ≈12 mCi of ^{11}C-PIB was injected i.v., and 60 min of dynamic PET scanning in 3D mode was initiated.

For each participant, ^{11}C-PIB images were aligned to each other and to the subject's magnetization-prepared 180° radio-frequency pulses and rapid gradient-echo image using an in-house cross-modal registration algorithm that minimizes the error function calculated from voxel-by-voxel activity levels, similar to maximizing the correlation matrixes (77). Alignment of the PET data then was computed using matrix multiplication, resulting in an atlas-transformed PET image resampled to 1-mm isotropic voxels. Registration was visualized in each participant to verify proper alignment.

Regional time–activity curves were analyzed for ^{11}C-PIB–specific binding using the Logan graphical analysis and the cerebellum data as a reference tissue input function (7). As an estimate of global brain Aβ accumulation, we used the mean cortical BP, which is an average of the gyrus rectus, lateral temporal, precuneus, and prefrontal cortex BP values, because these regions have ^{11}C-PIB uptake in individuals with DAT (7). BP values [mt]0.18 were considered abnormal (7, 78, 79).

Measurements of blood flow, glucose metabolism, and oxygen consumption are described in our companion paper (12).

ACKNOWLEDGMENTS. We thank Lenis Lich, Angela Jones, and Lori Groh for skilled technical assistance in PET scanning; Jon Christensen for help with data analysis; Abraham Z. Snyder for invaluable consultation on many aspects of data interpretation and analysis; the Washington University Alzheimer's Disease Research Center for participant assessment; and Sally Schwarz and the Washington University Cyclotron Facility for radiotracer production. This research was supported by National Institutes of Health Grants P50 AG05681, P50 NS006833, P20 MH077967, P01 AG003991, P30 NS048056, and F30 NS057901.

1. Mattson MP (2004) Pathways towards and away from Alzheimer's disease. *Nature* 430:631–639.
2. Hardy J, Selkoe DJ (2002) The amyloid hypothesis of Alzheimer's disease: Progress and problems on the road to therapeutics. *Science* 297:353–356.
3. Hulette CM, et al. (1998) Neuropathological and neuropsychological changes in "normal" aging: Evidence for preclinical Alzheimer disease in cognitively normal individuals. *J Neuropathol Exp Neurol* 57:1168–1174.
4. Morris JC, Price AL (2001) Pathologic correlates of nondemented aging, mild cognitive impairment, and early-stage Alzheimer's disease. *J Mol Neurosci* 17:101–118.
5. Klunk WE, et al. (2004) Imaging brain amyloid in Alzheimer's disease with Pittsburgh Compound-B. *Ann Neurol* 55:306–319.
6. Fagan AM, et al. (2006) Inverse relation between in vivo amyloid imaging load and cerebrospinal fluid Abeta42 in humans. *Ann Neurol* 59:512–519.
7. Mintun MA, et al. (2006) [11C]PIB in a nondemented population: Potential antecedent marker of Alzheimer disease. *Neurology* 67:446–452.
8. Raichle ME, et al. (2001) A default mode of brain function. *Proc Natl Acad Sci USA* 98: 676–682.
9. Buckner RL, et al. (2005) Molecular, structural, and functional characterization of Alzheimer's disease: Evidence for a relationship between default activity, amyloid, and memory. *J Neurosci* 25:7709–7717.
10. Raichle ME, Snyder AZ (2007) A default mode of brain function: A brief history of an evolving idea. *Neuroimage* 37:1083–1090, discussion 1097–1099.
11. Buckner RL, Andrews-Hanna JR, Schacter DL (2008) The brain's default network: Anatomy, function, and relevance to disease. *Ann N Y Acad Sci* 1124:1–38.
12. Vaishnavi SN, et al. (2010) Regional aerobic glycolysis in the human brain. *Proc Natl Acad Sci USA*, 10.1079/pnas1010459107.
13. Raichle ME, Posner JB, Plum F (1970) Cerebral blood flow during and after hyperventilation. *Arch Neurol* 23:394–403.
14. Boyle PJ, et al. (1994) Diminished brain glucose metabolism is a significant determinant for falling rates of systemic glucose utilization during sleep in normal humans. *J Clin Invest* 93:529–535.
15. Powers WJ, et al. (2007) Selective defect of in vivo glycolysis in early Huntington's disease striatum. *Proc Natl Acad Sci USA* 104:2945–2949.
16. Vander Heiden MG, Cantley LC, Thompson CB (2009) Understanding the Warburg effect: The metabolic requirements of cell proliferation. *Science* 324:1029–1033.
17. Bolanos JP, Delgado-Esteban M, Herrero-Mendez A, Fernandez-Fernandez S, Almeida A (2008) Regulation of glycolysis and pentose-phosphate pathway by nitric oxide: Impact on neuronal survival. *Biochim Biophys Acta* 1777 (7-8):789–793.
18. Vaughn AE, Deshmukh M (2008) Glucose metabolism inhibits apoptosis in neurons and cancer cells by redox inactivation of cytochrome c. *Nat Cell Biol* 10:1477–1483.

19. Jolivet R, Magistretti PJ, Weber B (2009) Deciphering neuron-glia compartmentalization in cortical energy metabolism. *Front Neuroenergetics* 1:1–10.
20. Minoshima S, Cross DJ, Foster NL, Henry TR, Kuhl DE (1999) Discordance between traditional pathologic and energy metabolic changes in very early Alzheimer's disease. Pathophysiological implications. *Ann N Y Acad Sci* 893:350–352.
21. Minoshima S, Foster NL, Kuhl DE (1994) Posterior cingulate cortex in Alzheimer's disease. *Lancet* 344:895.
22. Cohen AD, et al. (2009) Basal cerebral metabolism may modulate the cognitive effects of Abeta in mild cognitive impairment: An example of brain reserve. *J Neurosci* 29:14770–14778.
23. Rabinovici GD, et al. (2010) Increased metabolic vulnerability in early-onset Alzheimer's disease is not related to amyloid burden. *Brain* 133:512–528.
24. Reivich M, et al. (1979) The [^{18}F fluorodeoxyglucose method for the measurement of local cerebral glucose utilization in man. *Circ Res* 44:127–137.
25. Phelps ME, et al. (1979) Tomographic measurement of local cerebral glucose metabolic rate in humans with (F-18)2-fluoro-2-deoxy-D-glucose: Validation of method. *Ann Neurol* 6:371–388.
26. Mielke R, Herholz K, Grond M, Kessler J, Heiss WD (1994) Clinical deterioration in probable Alzheimer's disease correlates with progressive metabolic impairment of association areas. *Dementia* 5:36–41.
27. Minoshima S, et al. (1997) Metabolic reduction in the posterior cingulate cortex in very early Alzheimer's disease. *Ann Neurol* 42:85–94.
28. Fox PT, Raichle ME, Mintun MA, Dence C (1988) Nonoxidative glucose consumption during focal physiologic neural activity. *Science* 241:462–464.
29. Madsen PL, et al. (1995) Persistent resetting of the cerebral oxygen/glucose uptake ratio by brain activation: Evidence obtained with the Kety-Schmidt technique. *J Cereb Blood Flow Metab* 15:485–491.
30. Warburg O (1939) *The Metabolism of Tumors* (Constable & Company, London); trans Dickens F.
31. Brand KA, Hermfisse U (1997) Aerobic glycolysis by proliferating cells: A protective strategy against reactive oxygen species. *FASEB J* 11:388–395.
32. Elston GN, Oga T, Fujita I (2009) Spinogenesis and pruning scales across functional hierarchies. *J Neurosci* 29:3271–3275.
33. Tononi G, Cirelli C (2006) Sleep function and synaptic homeostasis. *Sleep Med Rev* 10: 49–62.
34. Marder E, Prinz AA (2002) Modeling stability in neuron and network function: The role of activity in homeostasis. *Bioessays* 24:1145–1154.
35. Altman DI, Perlman JM, Volpe JJ, Powers WJ (1993) Cerebral oxygen metabolism in newborns. *Pediatrics* 92:99–104.
36. Powers WJ, Rosenbaum JL, Dence CS, Markham J, Videen TO (1998) Cerebral glucose transport and metabolism in preterm human infants. *J Cereb Blood Flow Metab* 18: 632–638.
37. Settergren G, Lindblad BS, Persson B (1976) Cerebral blood flow and exchange of oxygen, glucose, ketone bodies, lactate, pyruvate and amino acids in infants. *Acta Paediatr Scand* 65:343–353.
38. Chugani HT, Phelps ME, Mazziotta JC (1987) Positron emission tomography study of human brain functional development. *Ann Neurol* 22:487–497.
39. Raichle ME, Mintun MA (2006) Brain work and brain imaging. *Annu Rev Neurosci* 29: 449–476.
40. Pellerin L, Magistretti PJ (1994) Glutamate uptake into astrocytes stimulates aerobic glycolysis: A mechanism coupling neuronal activity to glucose utilization. *Proc Natl Acad Sci USA* 91:10625–10629.
41. Mercer RW, Dunham PB (1981) Membrane-bound ATP fuels the Na/K pump. Studies on membrane-bound glycolytic enzymes on inside-out vesicles from human red cell membranes. *J Gen Physiol* 78:547–568.
42. Okamoto K, Wang W, Rounds J, Chambers EA, Jacobs DO (2001) ATP from glycolysis is required for normal sodium homeostasis in resting fast-twitch rodent skeletal muscle. *Am J Physiol Endocrinol Metab* 281:E479–E488.
43. Campbell JD, Paul RJ (1992) The nature of fuel provision for the Na+,K(+)-ATPase in porcine vascular smooth muscle. *J Physiol* 447:67–82.
44. Wu K, Aoki C, Elste A, Rogalski-Wilk AA, Siekevitz P (1997) The synthesis of ATP by glycolytic enzymes in the postsynaptic density and the effect of endogenously generated nitric oxide. *Proc Natl Acad Sci USA* 94:13273–13278.
45. Lipton P, Robacker K (1983) Glycolysis and brain function: [K+]o stimulation of protein synthesis and K+ uptake require glycolysis. *Fed Proc* 42:2875–2880.
46. McGilvery RW, Goldstein GW (1983) *Biochemistry: A Functional Approach* (Saunders, Philadelphia).
47. Olney JW (1969) Brain lesions, obesity, and other disturbances in mice treated with monosodium glutamate. *Science* 164:719–721.
48. Olney JW (2003) Excitotoxicity, apoptosis and neuropsychiatric disorders. *Curr Opin Pharmacol* 3:101–109.
49. Olney JW, Wozniak DF, Farber NB (1997) Excitotoxic neurodegeneration in Alzheimer disease. New hypothesis and new therapeutic strategies. *Arch Neurol* 54:1234–1240.
50. Irizarry MC, et al. (1997) Abeta deposition is associated with neuropil changes, but not with overt neuronal loss in the human amyloid precursor protein V717F (PDAPP) transgenic mouse. *J Neurosci* 17:7053–7059.
51. Palop JJ, Mucke L (2009) Epilepsy and cognitive impairments in Alzheimer disease. *Arch Neurol* 66:435–440.
52. Zhang D, et al. (2009) Na,K-ATPase activity regulates AMPA receptor turnover through proteasome-mediated proteolysis. *J Neurosci* 29:4498–4511.
53. Hsieh H, et al. (2006) AMPAR removal underlies Abeta-induced synaptic depression and dendritic spine loss. *Neuron* 52:831–843.
54. Seipp S, Buselmaier W (1994) Isolation of glyceraldehyde 3-phosphate dehydrogenase (Gapdh) cDNA from the distal half of mouse chromosome 16: Further indication of a link between Alzheimer's disease and glycolysis. *Neurosci Lett* 182:91–94.
55. Li Y, et al. (2004) Association of late-onset Alzheimer's disease with genetic variation in multiple members of the GAPD gene family. *Proc Natl Acad Sci USA* 101: 15688–15693.
56. Cumming RC, Schubert D (2005) Amyloid-beta induces disulfide bonding and aggregation of GAPDH in Alzheimer's disease. *FASEB J* 19:2060–2062.
57. Cirrito JR, et al. (2008) Endocytosis is required for synaptic activity-dependent release of amyloid-beta in vivo. *Neuron* 58:42–51.
58. Cirrito JR, et al. (2005) Synaptic activity regulates interstitial fluid amyloid-beta levels in vivo. *Neuron* 48:913–922.
59. Kamenetz F, et al. (2003) APP processing and synaptic function. *Neuron* 37:925–937.
60. Plant LD, et al. (2006) Amyloid beta peptide as a physiological modulator of neuronal 'A'-type K+ current. *Neurobiol Aging* 27:1673–1683.
61. Puzzo D, et al. (2008) Picomolar amyloid-beta positively modulates synaptic plasticity and memory in hippocampus. *J Neurosci* 28:14537–14545.
62. Lacor PN, et al. (2007) Abeta oligomer-induced aberrations in synapse composition, shape, and density provide a molecular basis for loss of connectivity in Alzheimer's disease. *J Neurosci* 27:796–807.
63. Freir DB, et al. (2010) Abeta oligomers inhibit synapse remodelling necessary for memory consolidation. *Neurobiol Aging*, S0 197-4580(10)00030-8[pii] doi: 10:1016/j.neurobiolaging.2010.01.001.
64. Mattson MP, Magnus T (2006) Ageing and neuronal vulnerability. *Nat Rev Neurosci* 7: 278–294.
65. Fukui H, Moraes CT (2008) The mitochondrial impairment, oxidative stress and neurodegeneration connection: Reality or just an attractive hypothesis? *Trends Neurosci* 31:251–256.
66. Mejias R, et al. (2006) Neuroprotection by transgenic expression of glucose-6-phosphate dehydrogenase in dopaminergic nigrostriatal neurons of mice. *J Neurosci* 26:4500–4508.
67. Russell RL, et al. (1999) Increased neuronal glucose-6-phosphate dehydrogenase and sulfhydryl levels indicate reductive compensation to oxidative stress in Alzheimer disease. *Arch Biochem Biophys* 370:236–239.
68. Soucek T, Cumming R, Dargusch R, Maher P, Schubert D (2003) The regulation of glucose metabolism by HIF-1 mediates a neuroprotective response to amyloid beta peptide. *Neuron* 39:43–56.
69. Palmer AM (1999) The activity of the pentose phosphate pathway is increased in response to oxidative stress in Alzheimer's disease. *J Neural Transm* 106:317–328.
70. Vulliamy T, Mason P, Luzzatto L (1992) The molecular basis of glucose-6-phosphate dehydrogenase deficiency. *Trends Genet* 8:138–143.
71. Magistretti PJ (2006) Neuron-glia metabolic coupling and plasticity. *J Exp Biol* 209: 2304–2311.
72. Herrero-Mendez A, et al. (2009) The bioenergetic and antioxidant status of neurons is controlled by continuous degradation of a key glycolytic enzyme by APC/C-Cdh1. *Nat Cell Biol* 11:747–752.
73. Allaman I, et al. (2010) Amyloid-beta aggregates cause alterations of astrocytic metabolic phenotype: Impact on neuronal viability. *J Neurosci* 30:3326–3338.
74. Allman J, Hakeem A, Watson K (2002) Two phylogenetic specializations in the human brain. *Neuroscientist* 8:335–346.
75. Craft S, et al. (1996) Memory improvement following induced hyperinsulinemia in Alzheimer's disease. *Neurobiol Aging* 17:123–130.
76. Morris JC (1993) The Clinical Dementia Rating (CDR): Current version and scoring rules. *Neurology* 43:2412–2414.
77. Snyder AZ (1996) Difference image vs ratio image error function forms in PET-PET realignment in quantification of brain function using PET. *Quantification of Brain Function Using PET*, eds Myer R, Cunningham VJ, Bailey DL, Jones T (Academic, San Diego), pp 131–137.
78. Fagan AM, et al. (2009) Cerebrospinal fluid tau and ptau(181) increase with cortical amyloid deposition in cognitively normal individuals: Implications for future clinical trials of Alzheimer's disease. *EMBO Mol Med* 1:371–380.
79. Morris JC, et al. (2010) APOE predicts amyloid-beta but not tau Alzheimer pathology in cognitively normal aging. *Ann Neurol* 67:122–131.